Optical Fiber Technology 34 (2017) 86–90

Contents lists available at ScienceDirect

Optical Fiber Technology

www.elsevier.com/locate/yofte

Bragg gratings in surface-core fibers: Refractive index and directional curvature sensing

Jonas H. Osório [a,*], Ricardo Oliveira [a,b], Stenio Aristilde [a], Giancarlo Chesini [a], Marcos A.R. Franco [c], Rogério N. Nogueira [b], Cristiano M.B. Cordeiro [a]

[a] Instituto de Física "Gleb Watagin", Universidade Estadual de Campinas, UNICAMP, Brazil
[b] Instituto de Telecomunicações, Pólo de Aveiro, Aveiro, Portugal
[c] Instituto de Estudos Avançados, IEAv, Departamento de Ciência e Tecnologia Aeroespacial, São José dos Campos, Brazil

ARTICLE INFO

Article history:
Received 26 September 2016
Revised 14 December 2016
Accepted 29 January 2017
Available online 7 February 2017

Keywords:
Bragg gratings
Curvature
Fiber tapers
Optical fibers
Refractive index
Sensors

ABSTRACT

In this paper, we report, to our knowledge, the first extended study of the inscription of Bragg gratings in surface-core fibers and their application in refractive index and directional curvature sensing. The research ranges from fiber fabrication and grating inscription in untapered and tapered fibers to the performance of simulations and sensing measurements. Maximum sensitivities of 40 nm/RIU and 202.7 pm/m^{-1} were attained in refractive index and curvature measurements respectively. The obtained results compares well to other fiber Bragg grating based devices. Ease of fabrication, robustness and versatility makes surface-core fibers an interesting platform when exploring fiber sensing devices.

1. Introduction

Optical fibers are a very important platform for building up sensors. Temperature, pressure, strain, refractive index and curvature are examples of parameters which can be monitored by the employment of optical fiber-based systems. The importance of developing fiber sensors has recently grown due to the advantages they can provide over other sorts of sensors, such as high sensitivity, electromagnetic immunity and increased robustness. Moreover, fiber-based devices are usually very compact and lightweight [1,2].

Numerous technologies can be employed for turning the fiber sensitive to the parameter whose variation is desired to be measured. Fiber gratings, for example, can be used to sense many parameters, such as refractive index, strain, curvature and temperature variations [3,4]. Furthermore, tailoring fiber geometry is another possibility for achieving the desirable sensitivity. It is often done when dealing with photonic crystal fibers [5].

Specifically for refractive index monitoring, long-period gratings [6,7], multimode interferometers devices (MMI) [8,9] and birefringent microfibers [10,11] are some of the fiber based devices that are usually employed for obtaining this sort of measurement. For these technologies, sensitivities values can range from hundreds to thousands of nanometers per refractive index unit.

Concerning curvature measurements, again long-period gratings and MMI based setups are often employed [12,13]. Moreover, Bragg gratings inscribed in multicore fibers have also been studied as an alternative for obtaining directional curvature determination [14–16].

In this paper, we report, to our knowledge, the first extended study of Bragg gratings inscribed in surface-core fibers and their application in refractive index and curvature probing. Surface-core fibers have firstly been reported by C. Guan et al. in [17], where theoretical studies of refractive index sensitivity can be found. Besides, an experimental study of refractive index sensing based on interferometry has also been published [18]. Recently, we have reported the fabrication and the possibility of inscribing long and short-period gratings in surface-core fibers [19]. Moreover, we studied the use of surface-core fibers for hydrostatic pressure sensing [20].

The research reported herein comprehends an investigation that ranges from fiber fabrication and simulation to its application in refractive index and directional curvature probing. When studying refractive index variations, a maximum sensitivity of 40 nm/RIU could be measured for refractive index variations around 1.42 RIU. Other fiber Bragg gratings devices reported in literature show sensitivity values ranging between 15 nm/RIU and 30 nm/

* Corresponding author.
E-mail address: jhosorio@ifi.unicamp.br (J.H. Osório).

http://dx.doi.org/10.1016/j.yofte.2017.01.007
1068-5200/

RIU [21–23]. Regarding curvature probing, a directional behavior was demonstrated and a sensitivity of 202.7 pm/m^{-1} could be attained. This value is two times higher than the values found in literature for similar FBG based sensors [14–16]. It's worth emphasizing that is not our intention reporting record high sensitivities values, but present the study of a specialty fiber structure obtained from a very simple fabrication process and its application in sensing measurements.

2. Fiber fabrication

Surface-core fibers are designed so that the core region is placed at fiber external boundary. In order to obtain the fiber, a four-step process is carried on. Firstly, a multimode germanium doped rod is drawn from its initial diameter of 21–0.8 mm (Fig. 1a). In the second step, the rod is inserted in a HF bath for etching. During this process, the diameter is decreased form 0.8 mm to 0.65 mm. By performing this procedure, the silica layer (Fig. 1a) is removed. This step is important for refractive index tests, since it allows a more pronounced interaction between the core mode evanescent field and the external medium.

In the third step, the thinned rod is merged to a silica tube (with inner and outer diameter of 5 mm and 10 mm, respectively) by the employment of a blowtorch in order to obtain the fiber preform (Fig. 1b). Finally, the preform is directly drawn to its final diameter (130 μm). The fiber cross-section is shown in Fig. 1c and a zoom of the core region is presented in Fig. 1d. As the core's refractive index is higher than the surrounding medium's one, light is guided through the surface-core fiber by total internal reflection.

It is worth underlining that all the steps for surface-core fiber fabrication are straightforward, what makes it much simpler than the fabrication of other specialty optical fibers such as photonic-crystal fibers. For obtaining photonic-crystal fibers, for instance, usually stack-and-draw procedure is employed [24]. In this method, numerous silica tubes and rods are drawn and manually assembled in a preform stack. In sequence, jacketing processes allows obtaining the desired proportion between core, cladding and outer fiber sizes. This process is very time consuming and demands much effort from a technical point of view.

3. Bragg gratings imprinting

Fiber Bragg gratings consist of short-period longitudinal modulation of optical fibers core refractive index. It allows coupling between forward and backward propagating core modes. The coupling occurs at a specific wavelength λ_B as shown in Eq. (1), where n_{eff} is the effective refractive index of the fundamental core mode and Λ is the grating period.

$$\lambda_B = 2n_{eff}\Lambda \quad (1)$$

The grating inscription was performed by employing the phase mask technique. A Quantel Q-Smart 450 UV laser together with a phase mask were used to create an FBG in the infrared region. A cylindrical lens was used for focusing the UV laser beam on the fiber during gratings' inscription process and the resulting FBGs have their lengths in the order of millimeters. For monitoring the FBG spectrum in real-time during grating inscription, a SMF pigtail was butt coupled to the surface core fiber. A small amount of index matching oil was used in the coupling for reducing Fresnel reflections at fiber ends and for lowering the background noise. A CCD camera was placed at the end of the fiber in order to provide an image of the core illumination conditions. By observing the CCD camera image, one could find the core position and optimize the coupling of light to the fiber. The FBGs were inscribed with enough reflectivity to be seen in reflection. Fig. 2a shows the spectrum (collected from a FS2200 Industrial BraggMETER from FiberSensing) of a FBG which was imprinted in a surface-core fiber by using a phase mask with period 1062.65 nm (spectra are normalized for better visualization). The tested fibers were maintained under tension during the gratings spectra acquisition.

4. Refractive index sensing

As in the studied fibers the core region is placed on fiber external surface, the evanescent field associated to the guided mode permeates the surrounding medium. It causes the core effective refractive index to be dependent on external refractive index variations. As the Bragg peak spectral location is determined, besides grating period, by the mode effective refractive index value (Eq. (1)), variations in external refractive index imply on Bragg peak shifting. Therefore, by monitoring the Bragg peak shift, a refractive index sensor can be obtained.

In the refractive index measurements, the surface-core fibers were immersed into solutions of water and glycerin and the reflection Bragg peak was monitored. Results showed, however, a very low sensitivity to external refractive index variations (0.07 nm/RIU). It can be identified by the minimum wavelength shift which was observed in Bragg peak spectral position as the external refractive index, n_{ext}, was varied (Fig. 2a). Thus, in order to enhance fiber sensitivity, tapers from surface-core fibers were produced prior to Bragg grating inscription. The tapers were prepared by using flame-brushing technique [25] and the grating imprinting was done by using the same phase-mask technique. In the flame-brushing technique, the resulting fiber taper presents two transition zones and a uniform region with constant diameter (taper waist). The gratings were imprinted in the uniform waist of the fiber tapers (prepared with 10 mm in length).

The diameter reduction causes the mode effective refractive index to be more sensitive to the surrounding refractive index variations. Tapers 80 μm and 20 μm thick were tested and the resulting spectra are shown in Fig. 2b and c (the spectra were normalized for better visualization). It is worth observing that the grating in the 80 μm taper was imprinted by using a phase mask with pitch 1075.34 nm and the one in the 20 μm with a phase mask with pitch 1071.2 nm, implying in different spectral positions for the Bragg peaks. Moreover, since the core mode in the 20 μm taper has a greater fraction of its evanescent field in the external med-

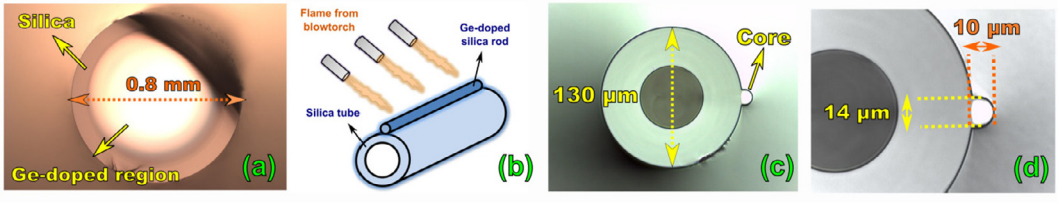

Fig. 1. (a) Germanium-doped silica preform employed for obtaining the fiber core. (b) Diagram for germanium doped silica rod and silica tube merging procedure using blowtorch. (c) Surface-core fiber cross-section. (d) Inset of the core region.

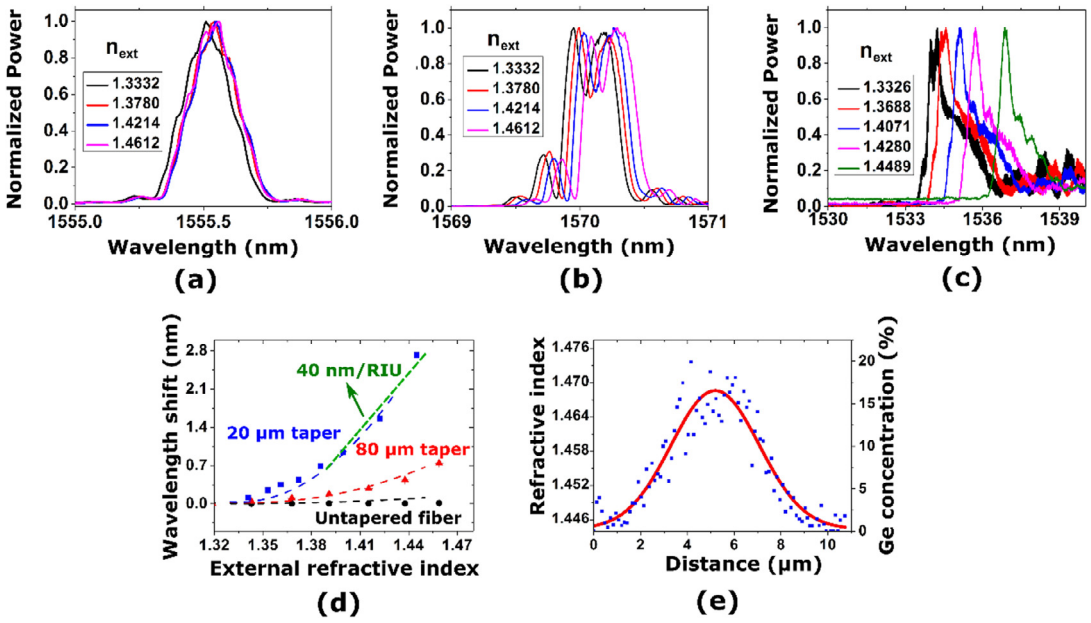

Fig. 2. Bragg gratings spectra in (a) untapered surface-core fiber and in (b) 80 μm and (c) 20 μm surface-core fiber tapers as a function of the external refractive index, n_{ext}. (d) Bragg wavelength shift as a function of external refractive index for untapered and tapered fibers. Dots stand for experimental data and dashed lines for simulations. (d) Core region refractive index and germanium concentration profile.

ium when compared to the 80 μm taper, the effective refractive index of the mode in the 20 μm taper is lower than the one in the 80 μm [22]. By observing Eq. (1), one can see that a lower effective refractive index causes the Bragg peak to appear at a lower wavelength.

Fig. 2d shows the wavelength shift as a function of the external refractive index for the untapered fiber (black circles) and for the 80 μm (red triangles) and 20 μm thick (blue squares) fiber tapers. It is seen that a greater wavelength shift is observed for the tapered fibers due to the more effective interaction between the core mode evanescent field and the surrounding medium. The sensitivity for refractive indexes around 1.42 RIU could be measured as 8 nm/RIU and 40 nm/RIU for the 80 μm and 20 μm thick fiber tapers respectively (Fig. 2d). Moreover, one can estimate, if an optical spectrum analyzer with 10 pm spectral resolution is used, the maximum sensor resolution as 2.5×10^{-4} RIU.

The maximum sensitivity value achieved for the surface-core fiber reported herein (40 nm/RIU, for a taper 20 μm thick) compares well with results from other authors who analyzed the shift of FBG fundamental mode. Ref. [21], for instance, reports a sensitivity of approximately 15 nm/RIU for a 6 μm taper in the refractive index range between 1.326 and 1.378 RIU. Besides, in Ref. [22], authors have found a value of 30 nm/RIU for a 8.5 μm taper in the same refractive index range. It can be observed that the results reported herein were obtained for thicker fiber tapers, which means an enhancement in sensor robustness.

Higher sensitivities values (in the order of hundreds or thousands of nm/RIU) are found in literature for setups based in other technologies such as fiber interferometers ([26,27]) and plasmonic devices [28]. Moreover, other approaches also using Bragg gratings in microfibers can be found in literature. For example, in Refs. [29] and [30], authors have monitored the FBG higher-order modes for achieving, respectively, maximum sensitivities of 92 nm/RIU and 102 nm/RIU around 1.38 RIU. In [29], a 7 μm taper was used and, in [30], a 6 μm thick one was employed. Moreover, a higher sensitivity can be found in [31] – 660 nm/RIU around 1.39 RIU – where the authors studied a FIB-milled Bragg grating induced on a 0.9 μm taper. These values were found, however, for very thin tapers, again reducing sensor robustness.

5. Fiber simulation

Numerical simulations were performed in order to corroborate experimental results. The fiber cross-section was initially drawn in a vector graphics editor (Corel Draw) in order to obtain a better reproduction of fiber geometry. In sequence, the drawing was imported into Comsol for mode analysis.

The core region of the surface core fibers is germanium doped and has a graded-index profile. Energy-dispersive X-ray spectroscopy technique (EDS) was employed for recovering the germanium concentration along the core region (Fig. 2e, right axis). By employing Eq. (2), where n is the refractive index of a germanium-doped silica glass at a concentration X and at a wavelength λ, it is possible to attain the refractive index of germanium-doped silica glass [32]. SA_i and SL_i, are the Sellmeier coefficients for silica (SiO_2) and GA_i and GL_i are the ones for germanium dioxide (GeO_2). Their values can be found in [32].

$$n^2 = 1 + \sum_{i=1}^{3} \frac{[SA_i + X(GA_i - SA_i)]\lambda^2}{\lambda^2 - [SL_i + X(GL_i - SL_i)]^2} \quad (2)$$

By using Eq. (2) and taking into account the germanium concentration distribution along the core, one obtained the core refractive index profile (Fig. 2e, left axis). A Gaussian function was fitted to the experimental data and the resulting curve (red line in Fig. 2e) was used for defining core refractive index in simulations, whose results are shown as dashed lines in Fig. 2d. As can be seen in Fig. 2d, good agreement is observed between simulated and experimental data.

6. Directional curvature sensing

In surface-core fibers, the core region is out of the center of symmetry. It makes the fiber able to probe directional curvature variations, since, depending on curvature direction, the fiber core experiences compression or expansion (Fig. 3a). In order to monitor curvature variations, a setup as depicted in Fig. 3b was used. Initially, the fiber containing the FBG was fixed between two rotator fiber holders (under straight condition). One of the stages on

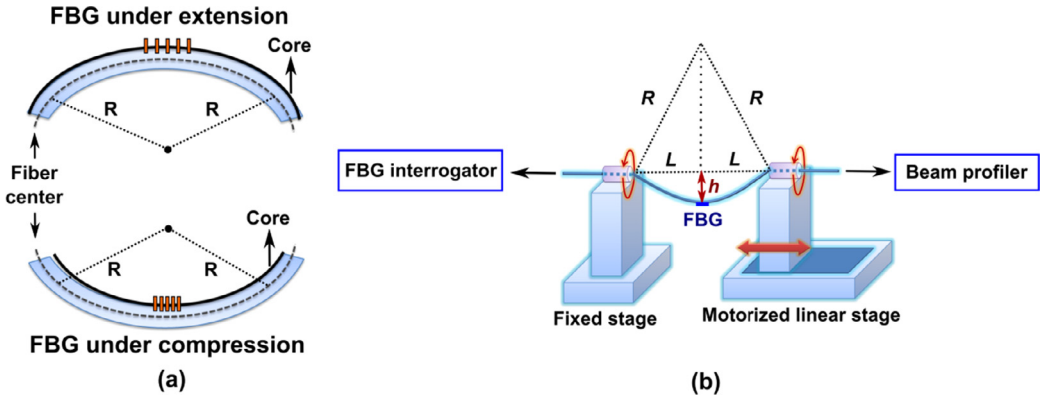

Fig. 3. (a) FBG is submitted to extension or compression depending on curvature direction. (b) Curvature sensing setup. *R*: curvature radius, 2*L*: bent length, *h*: distance from the straight position.

which the fiber was fixed was connected to a motorized stage whose linear movement towards the fixed stage implied on curvature increments.

In curvature sensing measurements, the curvature bending, *C*, is calculated as the inverse of the curvature radius (*R* in Fig. 3b) and is related to the displacement from the straight condition *h* by Eq. (3) – where 2*L* is the length of the bent fiber section [33].

$$C = \frac{1}{R} = \frac{2h}{h^2 + L^2} \tag{3}$$

For measuring directional curvature variations, care was taken in order of being sure that the curvature was being made on the right direction. Firstly, the fiber movement was limited to follow a single axis by keeping it between parallel plastic boards, following reference [33] authors' description. The second important point was being sure that the fiber had the right core orientation. To do that, a 50× magnification lens together with a beam profiler were used to monitor the core end face orientation at the region close to the fiber holder. Thus, by rotating the two fiber holders by the same angle, we could adjust the desired core orientation (see Fig. 3b).

For characterizing the response of the surface-core FBG to curvature variations, four configurations – different core orientation and bending direction – were tested. The investigated arrangements and the obtained results are summarized in Fig. 4. Green squares stands for grating under expansion and blue triangles for grating under compression. Red circles and pink rhombs are the results found for the situation in which the fiber was rotated 90° from the initial position (see Fig. 4).

In Fig. 4, one can observe that grating extension causes, as expected, the Bragg peak to redshift (positive wavelength shift). In contrast, grating compression causes the Bragg peak to blueshift (negative wavelength shift). Different wavelength shifting behavior shows the feasibility of using surface-core fiber for directional curvature probing. The results obtained for the situation in which the fiber was rotated (red circles and pink rhombs in Fig. 4) also followed the expected behavior (no curvature sensitivity is expected as the core is on the curvature neutral axis [33]). The observed small wavelength variations (within 0.35 nm) are due to possible misalignment between the grating axis and the bending plane.

The attained curvature sensitivities, 188.6 pm/m^{-1} and −202.7 pm/m^{-1}, are high when compared to other FBG bending sensors reported in literature (whose values range from 50 pm/m^{-1} to 100 pm/m^{-1}) [14–16]. They are also higher than the one found for FBG inscribed in eccentric core polymer fiber (63.3 pm/m^{-1} [33]). Other fiber configurations (not based in FBGs), can, however, provide increased curvature sensitivities. Two and three core optical fibers interrogated in interferometric setups are reported to attain sensitivities values as high as hundreds of nanometers per inverse meter [34,35].

7. Conclusion

To our knowledge, this paper is the first extended description of the study of FBGs inscribed in surface-core fibers and their application on refractive index and directional curvature sensing

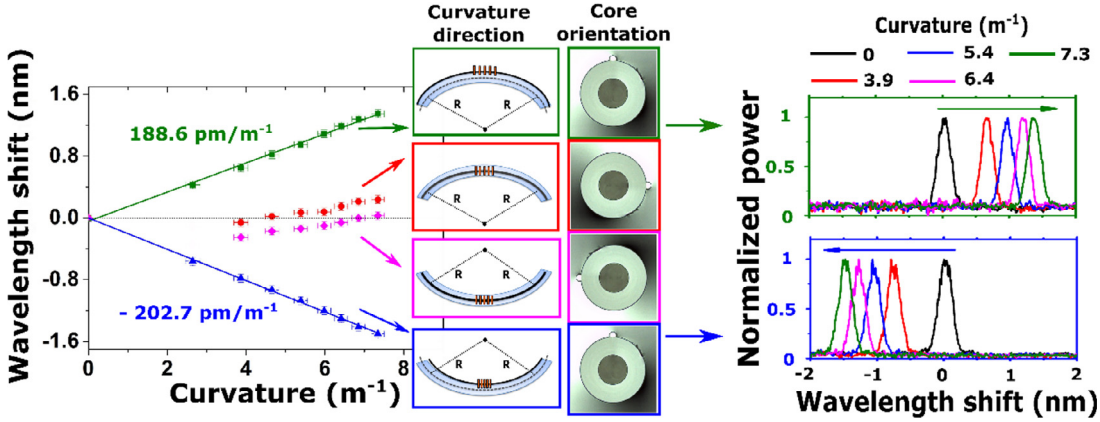

Fig. 4. Curvature sensing results. Green squares and blue triangles references FBG under extension and compression respectively. Red circles and pink rhombs are the results found after the fiber being rotated by 90°. Fitted lines are shown in green and blue. R: curvature radius. Spectra are shown for the grating expansion (top spectra) and grating compression (bottom spectra) experiments.

measurements. The research reported herein studied surface-core fibers from their fabrication to the performance of simulations and measurements of refractive index and curvature variations. It doesn't aim reporting record high sensitivities values but exposing the study of a new fiber structure which can be prepared by means of a very simple fabrication process and that can be applied in sensing measurements.

In the refractive index sensing experiments, a maximum sensitivity of 40 nm/RIU could be measured around 1.42 RIU. The obtained value compares well to other setups that monitor the spectral position of the FBG fundamental mode peak. Furthermore, the sensor reported herein has increased robustness when compared to other FBG-based refractive index sensors since a thicker fiber taper is employed (20 μm taper diameter).

In curvature probing, a directional behavior of the optical response could be observed due to the fiber geometry. A maximum sensitivity of 202.7 pm/m^{-1} was attained. This is also a good remark when compared to other FBG based curvature sensors reported in literature.

In conclusion, the results demonstrated the feasibility of the application of surface-core fibers on refractive index and directional curvature probing. Simple design, ease of fabrication, robustness and versatility makes this kind of fiber an interesting platform for the development of fiber-based devices for sensing purposes.

Acknowledgements

This research was funded by grant #2014/50632-6 from São Paulo Research Foundation (FAPESP) and FINEP (grant #01.12.0393.00). J. H. Osório acknowledges Conselho Nacional de Desenvolvimento Científico e Tecnológico (CNPq) and R. Oliveira acknowledges the National Funds through FCT-Fundação para a Ciência e Tecnologia under the project SFRH/BD/88472/2012 and UID/EEA/50008/2013 (Swat). The authors would like to thank J. A. Santos, A. C. Camillo and R. B. Borges for technical support.

References

[1] A.D. Kersey, A review of recent developments in fiber optic sensor technology, Opt. Fiber Technol. 2 (1996) 291–317.
[2] B. Lee, Review of the present status of optical fiber sensors, Opt. Fiber Technol. 9 (2003) 57–79.
[3] S.W. James, R.P. Tatam, Optical fibre long-period grating sensors: characteristics and application, Meas. Sci. Technol. 14 (2003) 49–61.
[4] Y.J. Rao, Recent progress in applications of in-fibre Bragg grating sensors, Opt. Lasers Eng. 31 (1999) 297–324.
[5] O. Frazão, J.L. Santos, F.M. Araújo, L.A. Ferreira, Optical sensing with photonic crystal fibers, Laser Photonics Rev. 2 (6) (2008) 449–459.
[6] H.J. Patrick, A.D. Kersey, F. Bucholtz, Analysis of the response of long period fiber gratings to external index od refraction, J. Lightwave Technol. 16 (9) (1998) 1606–1612.
[7] J.H. Osório, L. Mosquera, C.J. Gouveia, C.R. Biazoli, J.G. Hayashi, P.A.S. Jorge, C.M. B. Cordeiro, High sensitivity LPG Mach-Zehnder sensor for real-time fuel conformity analysis, Meas. Sci. Technol. 24 (2013) 1–8.
[8] S. Silva, E.G.P. Pachon, M.A.R. Franco, J.G. Hayashi, F.X. Malcata, O. Frazão, P. Jorge, C.M.B. Cordeiro, Ultrahigh-sensitivity temperature fiber sensor based on multimode interference, Appl. Opt. 51 (16) (2012) 3236–3242.
[9] C.R. Biazoli, S. Silva, M.A.R. Franco, O. Frazão, C.M.B. Cordeiro, Multimode interference tapered fiber refractive index sensors, Appl. Opt. 51 (24) (2012) 5941–5945.
[10] J. Li, L. Sun, S. Gao, Z. Quan, Y. Chang, Y. Ran, L. Jin, B. Guan, Ultrasensitive refractive-index sensors based on rectangular silica microfibers, Opt. Lett. 36 (18) (2011) 3593–3595.
[11] F. Beltrán-Mejía, J.H. Osório, C.R. Biazoli, C.M.B. Cordeiro, D-microfibers, J. Lightwave Technol. 31 (16) (2013) 3056–3061.
[12] H.J. Patrick, Self-aligning, bipolar bend transducer based on long period grating written in eccentric core fibre, Electron. Lett. 36 (21) (2000) 1763–1764.
[13] S. Silva, E.G.P. Pachon, M.A.R. Franco, P. Jorge, J.L. Santos, F.X. Malcata, C.M.B. Cordeiro, O. Frazão, Curvature and temperature discrimination using multimode interference fiber optic structures – a proof of concept, J. Lightwave Technol. 30 (23) (2012) 3569–3575.
[14] M.J. Gander, W.N. MachPherson, R. McBride, J.D.C. Jones, L. Zhang, I. Bennion, P. M. Blanchard, J.G. Burnett, A.H. Greenaway, Bend measurement using Bragg gratings in multicore fibre, Electron. Lett. 36 (2) (2000) 120–121.
[15] G.M.H. Flockhart, W.N. MacPherson, J.S. Barton, J.D.C. Jones, Two-axis bend measurement with Bragg gratings in multicore optical fiber, Opt. Lett. 28 (6) (2003) 387–389.
[16] F.M. Araújo, L.A. Ferreira, J.L. Santos, Simultaneous determination of curvature, plane of curvature, and temperature by use of a miniaturized sensing head based on fiber Bragg gratings, Appl. Opt. 41 (13) (2002) 2401–2407.
[17] C. Guan, L. Yuan, F. Tian, Q. Dai, Characteristics of near-surface-core optical fibers, J. Lightwave Technol. 29 (19) (2011) 3004–3008.
[18] X. Tian, C. Guan, H. Wu, L. Yuan, A refractive index sensor based on near-surface-core fiber, in: Proc. SPIE 8421, OFS2012 22nd International Conference on Optical Fiber Sensors, 84211R, 2012.
[19] J.H. Osório, R. Oliveira, L. Mosquera, M.A.R. Franco, J. Heidarialamdarloo, L. Bilro, R.N. Nogueira, C.M.B. Cordeiro, Surface-core fiber gratings, in: Proc. SPIE 9634, 24th International Conference on Optical Fibre Sensors, 96340V, 2015.
[20] J.H. Osório, M.A.R. Franco, Cristiano M.B. Cordeiro, Hydrostatic pressure sensing with surface-core fibers, in: Proc. SPIE 9634, 24th International Conference on Optical Fibre Sensors, 96343B, 2015.
[21] W. Liang, Y. Huang, Y. Xu, R.K. Lee, A. Yariv, Highly sensitive fiber Bragg grating refractive index sensors, Appl. Phys. Lett. 86 (2005) 151122.
[22] A. Iadicicco, A. Cusano, A. Cutolo, R. Bernini, M. Giordano, Thinned fiber Bragg gratings as high sensitivity refractive index sensor, IEEE Photonics Technol. Lett. 16 (4) (2004) 1149–1151.
[23] J. Kou, M. Ding, J. Feng, Y. Lu, F. Xu, G. Brambilla, Microfiber-based Bragg gratings for sensing applications: a review, Sensors 12 (2012) 8861–8876.
[24] P. Russell, Photonic crystal fibers, Science 299 (2003) 358–362.
[25] T.A. Birks, Y.W. Li, The shape of fiber tapers, J. Lightwave Technol. 10 (4) (1992) 432–438.
[26] T. Wei, Y. Han, Y. Li, H.-L. Tsai, H. Xiao, Temperature-insensitive miniaturized fiber inline Fabry-Perot interferometer for highly sensitive refractive index measurement, Opt. Express 16 (2008) 5764–5769.
[27] Y. Wang, M. Yang, D.N. Wang, S. Liu, P. Lu, Fiber in-line Mach-Zehnder interferometer fabricated by femtosecond laser micromachining for refractive index measurement with high sensitivity, J. Opt. Soc. Am. B: Opt. Phys. 27 (2010) 370–374.
[28] P. Bhatia, B.D. Gupta, Surface plasmon resonance based fiber optic refractive index sensor utilizing silicon layer: effect of doping, Opt. Commun. 286 (2013) 171–175.
[29] S. Lee, S.S. Saini, M. Jeong, Simultaneous measurement of refractive index, temperature and strain using etched-core fiber Bragg grating sensors, IEEE Photonics Technol. Lett. 22 (19) (2010) 1431–1433.
[30] Y. Zhang, B. Lin, S.C. Tjin, H. Zhang, G. Wang, P. Shum, X. Zhang, Refractive index sensing based on higher-order mode reflection of a microfiber Bragg grating, Opt. Express 18 (25) (2010) 26345–26350.
[31] Y. Liu, C. Meng, A.P. Zhang, Y. Xiao, H. Yu, L. Tong, Compact microfiber Bragg gratings with high index contrast, Opt. Lett. 36 (16) (2011) 3115–3117.
[32] J.W. Fleming, Dispersion in GeO_2-SiO_2 glasses, Appl. Opt. 23 (24) (1984) 4486–4493.
[33] X. Chen, C. Zhang, D.J. Webb, G. Peng, K. Kalli, Bragg grating in a polymer optical fibre for strain, bend and temperature sensing, Meas. Sci. Technol. 21 (2010) 094005.
[34] J. Villatoro, A.V. Newkirk, E. Antonio-Lopez, J. Zubia, A. Schülzgen, R. Amezcua-Correa, Ultrasensitive vector bending sensor based on multicore optical fiber, Opt. Lett. 41 (2016) 832–835.
[35] J.R. Guzman-Sepulveda, D.A. May-Arrioja, In-fiber directional coupler for high-sensitivity curvature measurement, Opt. Express 21 (2013) 11853–11861.